Journal of Thermal Analysis and Calorimetry (2021) 145:1585–1597
https://doi.org/10.1007/s10973-021-10833-z

Process design and thermoeconomic evaluation of a CO_2 liquefaction process driven by waste exhaust heat recovery for an industrial CO_2 capture and utilization plant

Reza Shirmohammadi[1,2] · Alireza Aslani[1] · Roghayeh Ghasempour[1] · Luis M. Romeo[3] · Fontina Petrakopoulou[2]

Received: 10 February 2021 / Accepted: 6 April 2021 / Published online: 13 May 2021

Abstract

Industrial surplus heat is a great available source and because of potential for external use can create benefits for society and industry. Utilizing surplus heat can deliver a way to decrease the use of primary energy and to play a part in global CO_2 mitigation. The potential of using excess heat in the main industrial CO_2 capture and utilization plant of Iran is investigated. A CO_2 liquefaction cycle i.e., ammonia-water absorption system is developed using the heat waste of the flue gas. Process modeling is developed in Aspen Hysys™ v.10 software with the aid of Peng-Robinson equation of state. Energy, exergy, economic and exergoeconomic analyses are then employed to evaluate the developed CO_2 liquefaction cycle integrated into the carbon capture and utilization plant. Results of process design and simulation show that the developed CO_2 liquefaction system can liquify CO_2 with the capacity of 54.5 tons per day using the flue gas enthalpy. The developed CO_2 liquefaction system has the COP of 0.28, and overall exergy efficiency of 69.7%. The highest amount of exergy is destructed in ammonia reboiler with the amount of 281.92 kW. Exergoeconomic results reveal that the compressors in CO_2 compression unit along with ammonia absorber and stripper have the highest importance among equipment.

Keywords CO_2 liquefaction · CCU · CO_2 capture · Absorption refrigeration · Process design

Abbreviations

ARS	Absorption refrigeration system
CCU	Carbon capture and utilization
CCUS	Carbon capture utilization and storage
EH	Excess heat
HR	Heat recovery

Symbols

C	Cost (USD)
ex	Specific exergy (J kg^{-1})
$\dot{E}_D$	Exergy destruction rate (kW)
$\dot{E}_f$	Fuel exergy rate (kW)
$\dot{E}_p$	Product exergy rate (kW)
h	Specific enthalpy (kJ kg^{-1})
K	Component
$\dot{m}$	Mass flow rate (kg s^{-1})
P	Pressure (kPa)
$\dot{Q}$	Rate of heat transfer (kW)
R	Universal gas constant (kJ $kmol^{-1}$ K^{-1})
S	Specific entropy (kJ kg^{-1} K^{-1})
T	Temperature (K)
V	Velocity (m s^{-1})
$\dot{W}$	Work transfer rate (kW)
$\dot{Z}$	Capital investment (USD)

Greek symbols

ε	Efficiency
φ	Maintenance factor
τ	Annual operating hours

Subscripts

0	Reference state condition (1 atm, 298 K)
1 2… 116	Points in Fig. 2
Ph	Physical exergy
Ch	Chemical exergy

✉ Reza Shirmohammadi
r.shirmohammadi@ut.ac.ir; rshirmoh@ing.uc3m.es

✉ Alireza Aslani
alireza.aslani@ut.ac.ir

[1] Department of Renewable Energy and Environment, Faculty of New Sciences & Technologies, University of Tehran, Tehran, Iran

[2] Department of Thermal and Fluid Engineering, University Carlos III of Madrid, Madrid, Spain

[3] Escuela de Ingeniería Y Arquitectura, Departamento de Ingeniería Mecánica, Universidad de Zaragoza, María de Luna 3, 50018 Zaragoza, Spain

D	Destruction
F	Fuel
P	Product
tot	Total

Superscripts

i	Number of components
n	Number of operation years

Introduction

The unceasing rise of CO_2 emission is a foremost reason for global warming. There are many methods existing for emission mitigation in expressive quantities, such as substituting fossil-based power generation plants with the renewable-based one, concentrating on efficiency enhancement of industrial and power plants, using carbon capture utilization and storage (CCUS) as a way of avoiding most of the CO_2 emission, while still using fossil fuels [1]. CCUS is a reliable CO_2 emission mitigation technology that can be applied across the energy system [2]. Industries have relayed on fossil fuels than electricity for their operation, mainly in developing countries. Furthermore, renewable technologies are capital-intensive, and their availability declines their competitiveness with fossil fuels in some scenarios. Consequently, fossil fuels have a vital role in the future energy mix of the world [3]. However, the former concept of carbon capture and storage (CCS) is no longer rational, and it has already been altered to CCUS, including direct utilization of CO_2 or its conversion by a chemical or biological process into a new product as well as long lasting application in enhanced oil and gas recovery [4].

Petrochemicals are considered as main blind spots in the global energy dispute, given the effect that the sector will apply on future energy trends. Inasmuch as the sector obtains far less attention than it deserves,attentions have been increased for optimum operation and design of energy-intensive industries such as petrochemicals during the last decades [5]. The need for a reduction in energy consumption and optimization in energy-intensive industries has been exposed with the increasing price of energy, a shortage of resources and environmental issues [6].

Energy-efficient utilization can yield improvement in a process or in a greater system in which the energy flows are integrated in the system. Several selections can be employed to take advantage of industrial excess heat (EH). The reduction in EH released by the processes as well as utilization in the industrial process i.e., heat recovery (HR), where it arose, are the best option and comparatively low-cost ways. This HR can be accomplished using a heat exchanger to preheat an incoming stream. Additionally, HR can be hired for external application. In this case, there would be heat losses; therefore, the HR must be situated adjacent to the heat source with a high heat exchange efficiency. HR results in several benefits such as reduction in both prime energy demand and CO_2 emission amounts. Industrial EH specification, i.e., quantity and quality, stipulate the possibility of HR. The former specify energy amount contained in the streams, whereas the latter measures stream potential in terms of its temperature [7]. The application of industrial EH utilization has been investigated in the literature e.g., [8–10]; nevertheless, it is claimed that a huge unexploited potential exists. The aim of energy efficiency and industrial EH utilization have drawn attention to the significance of HR and the deployment and development of such technologies [11].

Enhancing and appropriate application of absorption refrigeration systems (ARSs) have recently been of interest for industrial EH utilization. Lithium bromide-H_2O and ammonia-H_2O ARSs are considered as two of the most prominent ARSs [12]. Lithium bromide-H_2O ARS is mainly employed for moderate temperature application like Heating, ventilation, and air-conditioning systems, whereas, ammonia-H_2O ARS is mainly employed for low-temperature systems [13]. ARSs are driven chiefly by thermal energy with small or no need for power [14].

Several researches have been done for developing ARSs for reducing energy consumption and using waste exhaust HR in a variety of hybrid energy systems e.g., [15–17]. Chang et al. [18] investigated two kinds of distillation columns where the generator is substituted by the packed-bed tower in ARS. They found that the issue could increase the COP of the cycle because of the increased ammonia concentration in the vapor phase of the ammonia-water refrigerant. Ghorbani et al. [19] investigated the possibility of utilizing ARS instead of pre-cooling stage of mixed fluid cascade (MFC) refrigeration cycle in an integrated cryogenic refrigeration process in order to reduce the energy consumption of the plant. They employed the ammonia-water ARS to provide the primarily required cooling of the system in an integrated cryogenic process for natural gas liquefaction. They also presented and compared alternatives for providing the required heat for driving of the ARS.

Aliyon et al. [20] developed and compared four types of CO_2 liquefaction systems by means of thermoeconomical evaluations. They concluded that the integrated ARS performed better than of the other systems in terms of exergy efficiency, capital, operational, and life cycle costs.

Ghorbani et al. [21] investigated use of ARS instead of pre-cooling stage of MFC refrigeration cycle with the aim of energy consumption reduction. They found that the high amount of energy consumption in the developed structure reduced due to the possibility of using wasted energy of the plant. Utilizing ARS as an alternative to compression refrigeration system in the developed integrated structure declined specific power and capital cost significantly.

Shirmohammadi et al. [22] analyzed an ARS, integrated to a CO_2 capture unit, for HR from flue gas of a natural-gas-fired power plant. Ghorbani et al. [23] developed and analyzed a novel MFC natural gas liquefaction process. They replaced a water-ammonia ARS with one of the vapor-compression refrigeration cycles. Ghorbani et al. [24] developed an ARS as an alternative to the compression refrigeration system of MFC refrigeration with the aim of reduction in the required energy. High energy consumption in such units was declined because of the elimination of a stage of the compression system and using of waste heat through the ARS.

In this paper, in order to utilize from waste exhaust heat of the ammonia production plant, CO_2 liquefaction cycle, driven with EH of the ammonia plant stack, for developing of an industrial CCU plant is proposed. Next the ammonia absorption system is simulated in ASPEN Hysys using the data available in the literature and then the cycle is designed with specifications required for this study. Eventually, in order to evaluate the developed system, thermoeconomic assessment is conducted.

Case study

Iran has emitted a considerable amount of CO_2 over the past decades. Refineries and petrochemicals as well as power generations plants are considered the main emission sources. Petrochemicals can be considered as the primary priority for applying and coupling of CCU plants. Kermanshah Petrochemical Industries Co. (KPIC), situated in the western part of Iran, is involved in producing and marketing chemicals and agricultural fertilizers. In this complex, urea fertilizer, liquid ammonia, and liquid nitrogen have been produced. Ammonia is always in excess at urea production facilities. This issue shows that by capturing CO_2 from the ammonia plant's stack, stored ammonia can boost urea production, without the necessity to invest widely in major components such as reactors and reformers. In the KPIC, a post-combustion CO_2 capture process was established for the separation of CO_2 from the flue gas of the primary reformer stack of the ammonia plant. The project at KPIC was designed, licensed, and constructed by Shahrekord Carbon Dioxide Co. (SCD) to recuperate 132 metric tons per day (MTPD) of CO_2 from the stack. The project was started in 2013, and it lasted 20 months for operating. Using this technology has empowered KPIC to consume less natural gas by 21.1 million normal cubic meters (MNm^3) per year, along with the reduction of CO_2 emission of 40,000 tons annually. Consequently, the establishment of the CCU plant has boosted the production capacity by 5%, without any additional investment beyond the implementation of the plant [25].

Developing of CCU plant using CO_2 liquefaction cycle

Process description

In order to liquify a portion of the captured CO_2, an absorption chiller driven by the heat waste of the flue gas from the ammonia plant's stack is considered. Table 1 shows the composition of the flue gas stream. Sulfur from natural gas combustion is herein assumed to be negligible. In fact, the resulting SO_X is less than 5 ppm. When combustion flue gas is employed for HR, the temperature is not allowed to drop below the sulfur trioxide dew point [26].

Figure 1 shows the place of the developed CO_2 liquefaction cycle in red color through a block flow diagram including the existing plants in Kermanshah Petrochemical Industries Co. The flue gas from the ammonia plant at the temperature of 178 °C is transported to the CO_2 capture unit entrance, and it is entered into the ammonia reboiler. The flue gas delivers sufficient energy for the CO_2 liquefaction cycle, which is responsible for liquefying of carbon dioxide. The exhaust flue gas from ammonia reboiler, at a temperature of 130 °C, is delivered to the underneath section of Soda ash wash-direct contact column where cooling is done and Soda Ash is also injected and neutralizes the resulting acidic compounds. The ammonium hydrate solution, called rich ammonia, enters the pump from the bottom of the ammonia absorber column. The rich solution is preheated by passing through the ammonia-water rich-lean heat exchanger, and delivered to the top of the ammonia stripper column. It then is heated by the steam produced in the ammonia reboiler and gradually loses its ammonia. The released ammonia, along with a large amount of water vapor, moves toward the upper part of the ammonia stripper column and the lean solution is sent from the lower part of the column into the ammonia reboiler by passing through the ammonia-water rich-lean heat exchanger. The released ammonia gas exits from the top of the stripper and enters into the shell side of ammonia condenser and is converted into the liquid ammonia. The liquid is then pressurized by passing an expansion valve from 12.3 to 0.29 bar. The mixture of gas and low-pressure liquid at − 28 °C enters the ammonia evaporative tubes. On the other hand, the captured

Table 1 Composition of the flue gas stream

Substance	Mole fraction fraction
N_2	0.724
CO_2	0.0678
O_2	0.0326
H_2O	0.1756

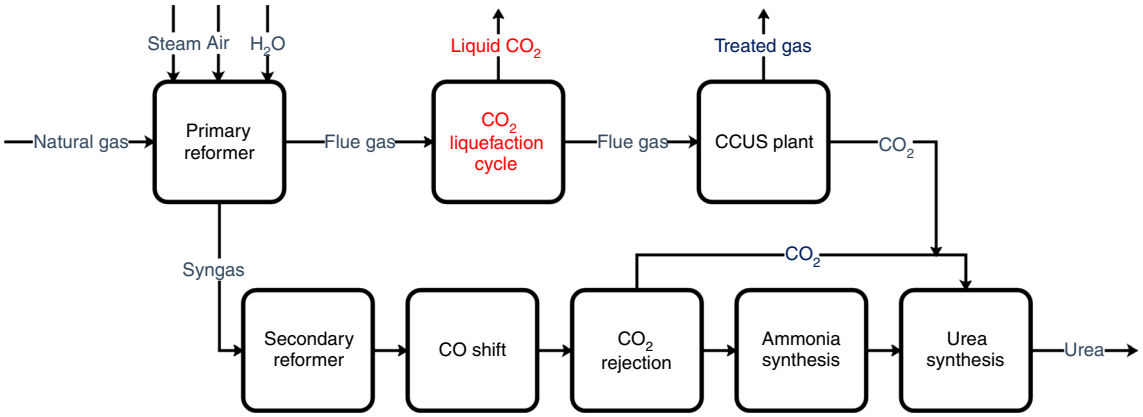

Fig. 1 Block flow diagram of the developed system among existing plants in the case study

CO_2 from the CCU plant is compressed in the two-stage compressors and its pressure increases up to 1605 kPa (CO_2 compression unit). Having passed through a cooler the compressed CO_2 declines its temperature up to 5 °C, and enters into the shell side of the evaporator and contacts with the surface of cool pipes, in which aqueous ammonia flows, and it finally is condensed. The purified liquid CO_2 overflows and is transferred to the storage tank. After evaporation, the ammonia gas enters the ammonia absorption column and is absorbed by the ammonia water solution. The lean solution from the ammonia reboiler is delivered to the upper part of the ammonia absorption column and absorbs ammonia gas throughout the column.

Simulation and thermodynamic framework

The modeling was developed in Aspen Hysys™ v.10 software using the Peng-Robinson equation of state. A significant benefit using the simulation software is the available models hired for thermodynamic properties. Various scientific articles have used the Peng-Robinson equation of state to design processes in the integrated structures. It is proven that the equation is accurate in a wide range of temperatures and pressures for predicting the properties of ammonia-water solution. Numerous references as design sources have been employed for the simulation of ammonia-water ARS. Somers [27] showed that the Peng-Robinson could be the best equation of state for simulation of water-ammonia ARS. Ghorbani et al. [19] and [28] also employed Peng-Robinson equation of state and Aspen Hysys simulation software to simulate the ARS. The ARS is primarily simulated by Hysys software with the aid of the available data in the literature. Then, the CO_2 liquefaction cycle is designed with conditions required into be integrated to the CCU plant.

Figure 2 shows a schematic of the developed CO_2 liquefaction cycle integrated into the CCU plant. The specifications of the inlet flue gas and outlet streams, including the liquified CO_2 and gaseous CO_2 are tabulated within the flow sheet of simulation. The liquified CO_2 is delivered to the storage tank, and the gaseous CO_2 is delivered to the urea plant. Table 2 shows thermodynamic properties of streams, which is designed for the developed CO_2 liquefaction cycle. NH3 mole fraction is also presented in Table 3 as one of the most important parameters in design and simulation of the system.

Table 4 shows equipment specifications of CO_2 liquefaction cycle. In the first section, the specification of the packed ammonia absorber and stripper columns including internal height, diameter, type, material, and dimension of each packed column, is provided. In the second part, separators are specified. In the third section, the specification of the pressure changer equipment, including differential pressure, pressure ratio, adiabatic efficiency, and consumed power, is provided. All of the aforementioned parameters are reported for the pump (P-100) and compressors of CO_2 compression unit; however, pressure ratio and drop are reported only for the expansion valve (VLV-100). In the last section, the specifications of the heat exchangers, i.e., NH_3 rich-lean heat exchangers (E-100), ammonia reboiler, ammonia condenser, evaporator and after coolers of CO_2 compression unit are provided.

Mathematical modeling

Thermoeconomic analysis is employed to evaluate the developed CO_2 liquefaction cycle integrated into the CCU plant. The analyses are explained in the following sections.

Energy analysis

The mass balance equation is written as below [29]:

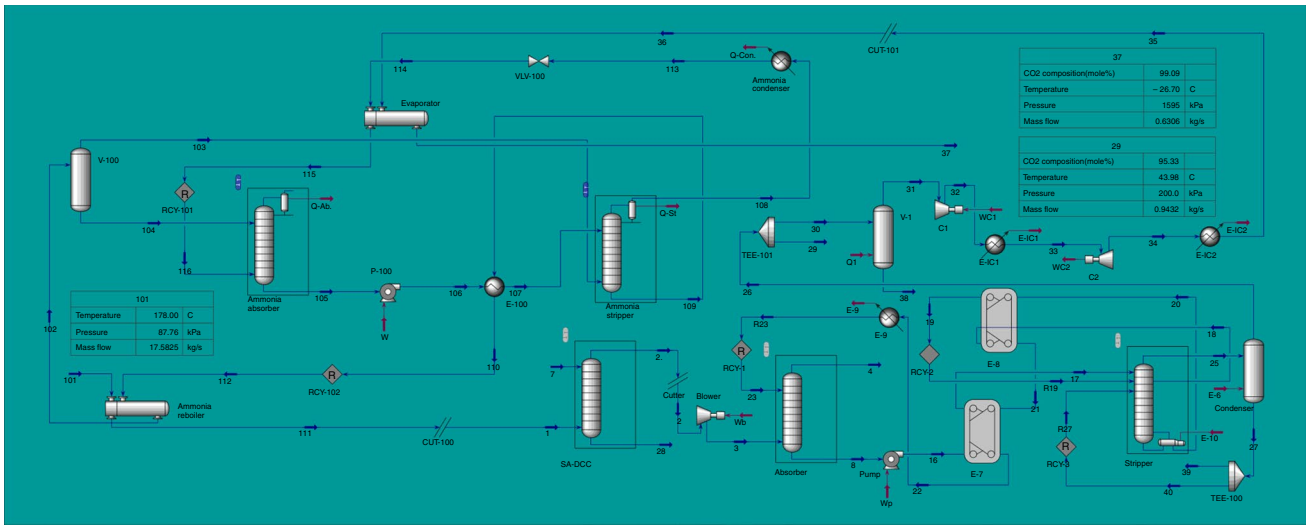

Fig. 2 Schematic of the developed CO2 liquefaction cycle integrated to the CCU plant

Table 2 Thermodynamic properties of streams

Stream no	Type of stream	Mass flow rate/kg/h	Temperature/°C	Pressure/kPa
101	Flue gas	63,297	178.0	87.8
102	NH3-H2O refrigerant	3575	115.4	1180.0
103	NH3-H2O refrigerant	890	115.4	1180.0
104	NH3-H2O refrigerant	2684	115.4	1180.0
105	NH3-H2O refrigerant	3460	−25.4	29.0
106	NH3-H2O refrigerant	3460	−25.2	1279.0
107	NH3-H2O refrigerant	3460	82.9	1270.0
108	Ammonia refrigerant	777	32.6	1250.0
109	NH3-H2O refrigerant	3573	84.0	1250.0
110	NH3-H2O refrigerant	3573	−20.7	1240.0
111	Flue gas	63,297	131.0	82.8
112	NH3-H2O refrigerant	3575	−20.7	1240.0
113	Ammonia refrigerant	777	31.4	1206.9
114	Ammonia refrigerant	777	−26.0	142.4
115	Ammonia refrigerant	777	−26.8	137.4
116	Ammonia refrigerant	777	−26.8	137.4
30	Captured CO2	2270	43	200
31	Gaseous CO2	2270	25	200
32	Gaseous CO2	2270	25	825
33	Gaseous CO2	2270	163	820
34	Gaseous CO2	2270	50	1605
35	Gaseous CO2	2270	5	1600.0
36	Gaseous CO2	2270	5	1600.0
37	Liquid CO2	2270	−26.7	1595.0
38	H2O	29.5	25	200

Table 3 NH3 mole fraction (%) for the developed ARS

Stream No	101	102	103	104	105	106	107	108	109	110	111	112	113	114	115	116
NH3 mole fraction (%)	0	0.42	0.89	0.26	0.44	0.44	0.44	1	0.42	0.42	0	0.42	1	1	1	1

Table 4 Equipment specification of CO2 liquefaction cycle and CO2 compression unit

Equipment	Specifications			
Column	Packing type	Packed diameter/[m]	Packed height/[m]	Material and dimension
Ammonia absorber	Pall	0.47	4	Metal, 1.5″
Ammonia stripper	Pall	0.35	3	Metal, 1.5″
Separators	Type	Vessel diameter/[m]	Height/[m]	Vessel volume/[m3]
V-100	Flat cylinder-vertical	0.6	3.3	0.97
V-1	Flat cylinder-vertical	1.1	3.7	3.3
Pressure changer	Pressure ratio	Adiabatic Efficiency	consumed power/[kW]	ΔP/[kPa]
P-100	44.1	75	1.88	1250
VLV-100	8.5	–	–	1064
C-1	4.125	75	80	625
C-2	1.95	75	36	780
Heat exchangers	(LMTD) / [°C]	Min. approach/[°C]	Shell-Tube ΔP/[kPa]	Heat duty/[kW]
Ammonia reboiler	76	65.5	50–5	687.5
Evaporator	2.1	1	5–5	192.4
E-100	2.4	1.1	10–9	474.2
Ammonia condenser	–	–	43	255.3
E-C1	–	–	5	77
E-C2	–	–	5	67

$$\sum_{\text{in}} \dot{m} = \sum_{\text{out}} \dot{m} \tag{1}$$

where $\dot{m}$ is the mass flow rate, and subscripts in and out shows the inlet and outlet streams. The energy balance equation is written as below [29]:

$$\dot{Q} + \sum_{\text{in}} \dot{m}\left(h + \frac{V^2}{2} + gZ\right) = \sum_{\text{out}} \dot{m}\left(h + \frac{V^2}{2} + gZ\right) + \dot{W} \tag{2}$$

where $\dot{W}$ and $\dot{Q}$ are the power and heat transfer rate; h depicts the specific enthalpy, and V shows velocity, g shows the gravitational acceleration, and Z is the height.

The coefficient of performance (COP) is defined as the ratio of the cooling load to the energy provided for the refrigeration system. The evaporator, which is transferred the cooling duty i.e., the enthalpy difference of the streams incoming and departing, is measured to be the refrigeration or cooling load, and the required thermal load provided for the CO_2 liquefaction cycle is given energy. Therefore, it is defined as follows:

$$\text{COP} = \frac{Q_{\text{C}}}{Q_{\text{H}} + W_{\text{P}}} \tag{3}$$

where Q_{C} is the refrigeration load of the evaporator, W_{P} is the pumping power, Q_{H} is the thermal energy of ammonia reboiler given to the CO_2 liquefaction cycle. The amount of COP considering heat duties of the evaporator and ammonia reboiler as well as consumed power of the pump presented values in Table 4 is being calculated. The COP for the CO_2 liquefaction cycle is equal to 0.28.

Exergy analysis

Exergy analysis is a gainful method, inasmuch as it reveals the locations, types, and real magnitudes of irreversibility either to be improved or inevitably lost. By assuming that there is no potential and kinetic energy, exergy of stream has been divided into physical and chemical exergy [30]. Physical exergy is equal to the maximum value of work available when the stream of a material is brought from

the actual state to the dead state which is defined by P0 and T0. It is depicted as [31]

$$e^{ph} = \left(h - h_0\right) - T_0\left(s - s_0\right) \tag{4}$$

In the above equation, e^{ph} is the specific physical exergy, h and s are, respectively, the specific enthalpy and entropy and $h_0 = f(T_0, P_0)$ and $s_0 = s(T_0, P_0)$. The molar chemical exergy of an ideal mixture is expressed as [31]:

$$e^{ch} = \sum x_i e_0^i + T_0 R \sum x_i \ln x_i \tag{5}$$

where x_i and e_0^i are, respectively, molar fraction and chemical exergy for every one of components in the mixture, and R is also the universal gas constant [31]. Values of standard chemical exergy (kJ mol^{-1}) are presented in the [32] and is for O_2, 3.97; N_2, 0.72; CO_2, 19.48; NH_3, 337.9; and liquid H_2O, 900.

For real solutions, the exergy of a mixture can be gained where activity coefficients i.e., Υ_i are recognized for the components. The more general version of Eq. 5:

$$e^{ch} = \sum x_i e_0^i + T_0 R \sum x_i \, ln \, x_i \, y_i \tag{6}$$

On the other hand, specific exergy of the chemical in the mixture can be achieved by the following equation.

$$e^{ch} = \sum x_i e_o^i \tag{7}$$

However, intermolecular forces difference needs to be measured for a real mixture. Thus, the following equation is employed.

$$e^{ch} = \sum \left(x_i e_o^i\right) + \Delta G^{mix} \tag{8}$$

Gibbs free energy is attained as follows.

$$\Delta G^{mix} = G - \sum x_i G_i \tag{9}$$

In this paper, the Gibbs free energy is employed to calculate exergy values of the streams. Table 5 shows the physical and chemical exergy values of streams existing in the CO_2 liquefaction cycle.

Exergy efficiency is a significant value resulting from the stream exergy analysis, defined in numerous formulations for diverse processes. It is defined as the ratio of the useful exergy output to the total input exergy [31]:

$$\varepsilon = \frac{\dot{E}_P}{\dot{E}_F} \tag{10}$$

where $\dot{E}_P$ and $\dot{E}_F$ stand for product and fuel part of exergy. The exergy destruction rate i.e., $\dot{E}_D$ for a component is written as: (10)

Table 5 Exergy value of the process streams

Stream no.	Physical exergy/(kW)	Chemical exergy/(kW)	Total exergy/(kW)
101	635.6	740.9	1376.5
102	151.5	8099.72	8254.24
103	90.5	4256.115	4347.652
104	39.2	3864.653	3904.6
105	36.8	8028.2	8065.1
106	38.4	8028.2	8066.6
107	39.6	8028.2	8067.8
108	75.9	4282.4	4358.3
109	39.0	7992.7	8031.7
110	33.5	7992.7	8026.3
111	33.5	7992.7	8026.3
112	69.5	8099.72	4351.9
113	61.8	4282.4	4344.2
114	21.1	4282.4	4303.5
115	21.1	4282.7	4303.8
116	255.7	740.9	996.6
30	25.3	279.2	304.5
31	24.1	277.2	301.3
32	88.2	277.2	365.5
33	74.1	277.2	351.3
34	103.1	277.2	380.3
35	98.3	277.2	375.5
36	98.3	277.2	375.5
37	137.2	277.2	414.4
38	0.001	2.0	2.0

$$\dot{E}_D = \dot{E}_F - \dot{E}_P - \dot{E}_L \tag{11}$$

The expression for the exergy rate due to heat transfer is as follows:

$$\dot{E}_Q = \dot{Q}\left(1 - \frac{T_0}{T}\right) \tag{12}$$

where the $\dot{Q}$ is heat rate [33].

Table 6 shows the exergy rate balances for components of the proposed system.

Exergoeconomic analysis

The economic evaluation of CO_2 liquefaction cycle including capital and operational costs is conducted using Aspen Process Economic Analyzer® (APEA). Capital costs typically encompass purchased equipment cost (PEC) and their installation costs, along with slight costs for electrical, instrumentation, piping, and building amenities, while operational costs generally consist of utility costs. APEA is a package to estimate equipment cost of a chemical process and is provided for both

Table 6 Balances of exergetic parameters for each component

Component	Fuel equations	Product equations	Destruction/Loss equations
Ammonia absorber	$\dot{E}_{F,Ab} = \dot{E}_{116}$	$\dot{E}_{P,Ab} = \dot{E}_{105} + \dot{E}_{Q,Ab} - \dot{E}_{104}$	$\dot{E}_{D,Ab} = \dot{E}_{F,Ab} - \dot{E}_{P,Ab}$
P-100	$\dot{E}_{F,P} = W_P$	$\dot{E}_{P,P} = \dot{E}_{106} - \dot{E}_{105}$	$\dot{E}_{D,P} = \dot{E}_{F,P} - \dot{E}_{P,P}$
Ammonia stripper	$\dot{E}_{F,St} = \dot{E}_{107} + \dot{E}_{103} - \dot{E}_{109}$	$\dot{E}_{P,St} = \dot{E}_{108} + \dot{E}_{Q,St}$	$\dot{E}_{D,St} = \dot{E}_{F,St} - \dot{E}_{P,St}$
E-100	$\dot{E}_{F,E-100} = \dot{E}_{109} - \dot{E}_{110}$	$\dot{E}_{P,E-100} = \dot{E}_{107} - \dot{E}_{106}$	$\dot{E}_{D,E-100} = \dot{E}_{F,E-100} - \dot{E}_{P,E-100}$
Ammonia condenser	$\dot{E}_{F,E-102} = \dot{E}_{108} - \dot{E}_{113}$	–	$\dot{E}_{D,E-102} = \dot{E}_{108} - \dot{E}_{113} - \dot{E}_{Q,Con.}$
Evaporator	$\dot{E}_{F,Eva.} = \dot{E}_{115} - \dot{E}_{114}$	$\dot{E}_{P,Eva.} = \dot{E}_{37} - \dot{E}_{36}$	$\dot{E}_{D,Eva.} = \dot{E}_{F,Eva.} - \dot{E}_{P,Eva.}$
Ammonia reboiler	$\dot{E}_{F,Reb.} = \dot{E}_{101} - \dot{E}_{111}$	$\dot{E}_{P,Reb.} = \dot{E}_{102} - \dot{E}_{112}$	$\dot{E}_{D,Reb.} = \dot{E}_{F,Reb.} - \dot{E}_{P,Reb.}$
V − 100	$\dot{E}_{F,V-100} = \dot{E}_{102}$	$\dot{E}_{P,V-100} = \dot{E}_{103} + \dot{E}_{104}$	$\dot{E}_{D,V-100} = \dot{E}_{F,V-101} - \dot{E}_{P,V-101}$
VLV-100	$\dot{E}_{F,VLV-100} = \dot{E}_{113} - \dot{E}_{114}$	–	$\dot{E}_{D,VLV-100} = \dot{E}_{113} - \dot{E}_{114}$
V-1	$\dot{E}_{F,V-1} = \dot{E}_{30}$	$\dot{E}_{P,V-1} = \dot{E}_{31} + \dot{E}_{38}$	$\dot{E}_{D,V-1} = \dot{E}_{F,V-1} - \dot{E}_{P,V-1}$
C1	$\dot{E}_{F,C1} = W_{C1}$	$\dot{E}_{P,C1} = \dot{E}_{32} - \dot{E}_{31}$	$\dot{E}_{D,C1} = \dot{E}_{F,C1} - \dot{E}_{P,C1}$
E-C1	$\dot{E}_{F,E-C1} = \dot{E}_{32} - \dot{E}_{33}$	–	$\dot{E}_{D,E-C1} = \dot{E}_{32} - \dot{E}_{33} - \dot{E}_{Q,E-C1.}$
C2	$\dot{E}_{F,C2} = W_{C2}$	$\dot{E}_{P,C2} = \dot{E}_{34} - \dot{E}_{33}$	$\dot{E}_{D,C2} = \dot{E}_{F,C2} - \dot{E}_{P,C2}$
E-C2	$\dot{E}_{F,E-C2} = \dot{E}_{34} - \dot{E}_{35}$	–	$\dot{E}_{D,E-C2} = \dot{E}_{34} - \dot{E}_{35} - \dot{E}_{Q,E-C2.}$
Overall ARS	$\dot{E}_{F,tot} = W_P + \dot{E}_{36} + \dot{E}_{F,Reb.}$	$\dot{E}_{P,tot} = \dot{E}_{37} + \dot{E}_{Q,St} + \dot{E}_{Q,Ab}$	$\dot{E}_{D,Total} = \dot{E}_{P,tot} - \dot{E}_{F,tot}$

simulated process in Aspen Hysys® and Aspen Plus® [34]. There are a couple of advantages for using APEA instead of correlation-based economic approaches. APEA has taken more parameters into account to estimate the cost of equipment than the correlation-based equations. As an illustration for heat exchangers, the impact of utilizing diverse materials, type, area and operating conditions has been considered by APEA for accurate cost estimation. Additionally, APEA takes the nature of installation cost into account, thus, installation costs are obtained precisely. For instance, pressure changer equipment has less installation cost than columns or heat exchangers, which is fairly rational [20]. In this study, the project type is selected to be plant addition-adjacent to existing plant, as the developed CO_2 liquefaction cycle is integrated with the CCU plant. Asia is selected for the location of the project, and USD is considered for the currency. Although Pre-engineered (standard) U tube exchanger is suggested for small-scale heat exchangers similar to the exchangers presented in the developed system, the heat exchangers are selected among common heat exchangers i.e., shell and tube and plate exchangers. Table 7 shows PEC as well as total direct

Table 7 PEC and TDC of the process equipment

Equipment tag	Equipment type ModMmtype	Equipment description	PEC/(USD) U(USD)	TDC/(USD)
Ammonia absorber	DTW PACKED	Packed tower	37,100	143,400
Condenser of absorber	DHE TEMA EXCH	TEMA shell and tube exchanger	14,200	141,800
Ammonia stripper	DTW PACKED	Packed tower	22,100	103,700
Condenser of stripper	DHE TEMA EXCH	TEMA shell and tube exchanger	10,400	67,300
Evaporator	DHE TEMA EXCH	TEMA shell and tube exchanger	30,600	134,500
E-100	DHE PLAT FRAM	Plate and frame heat exchanger	28,800	174,800
V-100	DVT CYLINDER	Vertical process vessel	16,200	95,700
Ammonia reboiler	DHE TEMA EXCH	TEMA shell and tube exchanger	29,800	121,300
Condenser	DHE TEMA EXCH	TEMA shell and tube exchanger	10,100	60,100
P-100	DCP CENTRIF	Centrifugal single or multi-stage pump	15,800	28,900
V-1	DVT CYLINDER	Vertical process vessel	15,300	91,700
C1	DGC CENTRIF	Centrifugal compressor	727,600	858,700
E-C1	DHE PLAT FRAM	Plate and frame heat exchanger	8500	59,100
C2	DGC CENTRIF	Centrifugal compressor	658,100	778,100
E-C2	DHE PLAT FRAM	Plate and frame heat exchanger	10,200	69,400

cost (TDC), including total material and manpower cost of the developed CO_2 liquefaction cycle's equipment.

The reported costs by APEA were updated in the release AspenONE V10 on 5th June 2017, consequently, the costs are updated for 2020. The updated costs in any reference date to another one [35]:

$$\text{Costat reference year} = \text{Original Cost} \times \frac{\text{CEPCI}_{\text{reference}}}{\text{CEPCI}_{\text{Original}}} \quad (13)$$

Chemical Engineering Plant Cost Index (CEPCI) is employed to update the equipment costs to different years [36]. CEPCI is updated and reported every month, consequently the CEPCI changes for short periods can be tracked as it is considered in the present study. The value of CEPCI index for 2020 is equal to 596.2 derived from the latest magazine of Chemical Engineering essentials for the global chemical processing industries. Figure 3 shows the increasing trend of CEPCI values during the five decades between 1960 and 2020.

The exergoeconomic evaluation employs the exergy unit cost and rate of cost for the all exergy streams to compute different variable of exergoeconomic for every one of devices of a system. For the system' component, the following cost balance is applied [37]:

$$\sum_{\text{out}=1}^{\text{m}} \dot{C}_{\text{out.k}} + \dot{C}_{\text{W.k}} = \sum_{\text{in}=1}^{\text{m}} \dot{C}_{\text{in.k}} + \dot{C}_{\text{Q.k}} + \dot{Z}_{\text{k}} \quad (14)$$

$\dot{Z}_{\text{K}}$ in the above equation signifies the cost rate of component k and encompasses $\dot{Z}_{\text{CI,K}}$ and $\dot{Z}_{\text{OM,K}}$ which represent the levelized capital investment and operating & maintenance costs, respectively. Furthermore, $\dot{Z}_{\text{K}}$ due to inflation is being corrected to the reference year 2020 as follows [38]:

$$\dot{Z}_{\text{K}} = \frac{\text{CEPCI}_{2020}}{\text{CEPCI}_{2017}} \times \frac{\text{CRF} \times \varphi}{\tau} \times \text{PEC}_{\text{K}} \quad (15)$$

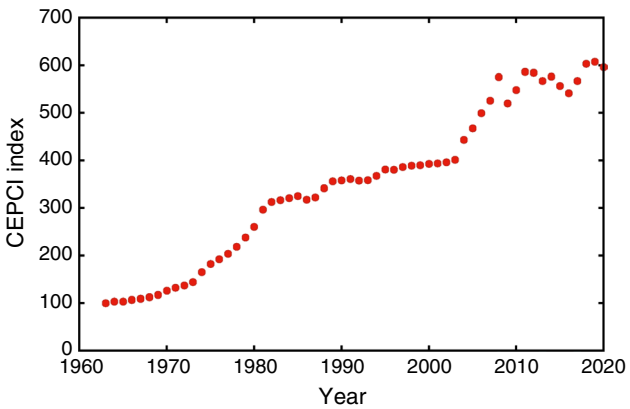

Fig. 3 CEPCI values during the five decades between 1960 and 2020

$$\text{CRF} = \frac{i(1+i)^{\text{n}}}{(1+i)^{\text{n}} - 1} \quad (16)$$

In the above equations, CRF stands for the capital recovery factor, φ is the maintenance factor and considered to be 1.06 [39], τ is the annual operating hours which is considered to be 8000 h, i is the interest rate, which is considered to be 10%, n which is the number of operation years is considered to be for 20 years [38], and PEC which is the purchase equipment cost which is obtained by the APEA.

The unit average of fuel exergy cost denotes the cost that the unit fuel exergy is provided for the K_{th} system' device. As a result, the following equation is stated [31]:

$$c_{\text{F,K}} = \dot{C}_{\text{F,K}} / \dot{E}_{\text{F,K}} \quad (17)$$

Likewise, the product unit cost $c_{\text{p,k}}$ is expressed as follows [31]:

$$c_{\text{P,K}} = \dot{C}_{\text{P,K}} / \dot{E}_{\text{P,K}} \quad (18)$$

The cost rate of each component i.e., $\dot{C}_{\text{D,K}}$ which is associated with the exergy destruction $\dot{E}_{\text{D,K}}$ of each component can be evaluated using the following equation [31]:

$$\dot{C}_{\text{D,K}} = c_{\text{F,K}} \dot{E}_{\text{D,K}} \quad (19)$$

Table 8 shows cost rate balances and auxiliary equations for each component. The cost rates of the utilities are obtained by APEA. Cost of electrical power used in compressors and the only pump of the system is equal to 21 \$ GJ^{-1}. The cost of thermal energy is equal to 2.89 \$ GJ^{-1}, and the cost cooling for dissipative equipment provided by cooling water is considered to be equal to 0.21 \$ GJ^{-1}.

The exergoeconomic factor i.e., f_{k} signifies the investment cost $\dot{Z}_{\text{k}}$ ratio over the multiplication of the unit fuel exergy cost to the sum of the exergy destruction and exergy cost, plus the $\dot{Z}_{\text{k}}$.

$$\frac{\dot{Z}_{\text{k}}}{\dot{Z}_{\text{k}} + C_{\text{F,K}} \times \left(\dot{E}_{\text{D,k}} + \dot{E}_{\text{L,k}}\right)} \quad (20)$$

The exergoeconomic factor also defines in absent of the lost exergy cost as the ratio of the investment cost to the sum of the investment as well as the exergy destruction cost [40].

$$f_{\text{k}} = \frac{\dot{Z}_{\text{k}}}{\dot{Z}_{\text{k}} + \dot{C}_{\text{D,K}}} \quad (21)$$

Exergoeconomic variable such as $\dot{Z}_{\text{k}} + \dot{C}_{\text{D,K}}$ provides an absolute criterion for the degree of importance of the K_{th} component, where as f_{k} propose relative criteria to assess the economic performance of a component.

Table 8 Cost rate balances and auxiliary equations for components of the proposed system

Component	Cost rate equations	Auxiliary equations
Ammonia absorber	$\dot{C}_{104} + \dot{C}_{116} + \dot{Z}_{\text{Ab.}} = \dot{C}_{105} + \dot{C}_{\text{Q,Ab.}}$	$c_{\text{Q,Ab.}}$
P-100	$\dot{C}_{30} + \dot{C}_{\text{W,Pump}} + \dot{Z}_{\text{Pump3}} = \dot{C}_{31}$	$c_{\text{W,Pump}}$
Ammonia stripper	$\dot{C}_{103} + \dot{C}_{107} + \dot{Z}_{\text{St.}} = \dot{C}_{108} + \dot{C}_{109} + \dot{C}_{\text{Q,St.}}$	$c_{\text{Q,St.}}$
E-100	$\dot{C}_{106} + \dot{C}_{109} + \dot{Z}_{\text{E-100}} = \dot{C}_{107} + \dot{C}_{110}$	$c_{109} = c_{110}$
Ammonia condenser	$\dot{C}_{108} + \dot{C}_{\text{Q,Cond.}} + \dot{Z}_{\text{Cond.}} = \dot{C}_{113}$	$c_{\text{Q,Cond.}}$
Evaporator	$\dot{C}_{36} + \dot{C}_{114} + \dot{Z}_{\text{Eva.}} = \dot{C}_{37} + \dot{C}_{115}$	$c_{114} = c_{115}$
Ammonia reboiler	$\dot{C}_{101} + \dot{C}_{112} + \dot{Z}_{\text{HTR}} = \dot{C}_{111} + \dot{C}_{102}$	$c_{101} = c_{111}$
V-100	$\dot{C}_{102} + \dot{Z}_{\text{V-100}} = \dot{C}_{103} + \dot{C}_{104}$	$c_{103} = c_{104}$
VLV-100	$\dot{C}_{114} - \dot{C}_{113} = 0$	–
V-1	$\dot{C}_{30} + \dot{Z}_{\text{V-1}} = \dot{C}_{31} + \dot{C}_{38}$	$c_{31} = c_{38}$
C1	$\dot{C}_{31} + \dot{C}_{\text{W,Comp1}} + \dot{Z}_{\text{Comp1}} = \dot{C}_{32}$	$c_{\text{W,Comp1}}$
E-C1	$\dot{C}_{32} + \dot{C}_{\text{Q, E-C1}} + \dot{Z}_{E-C1} = \dot{C}_{33}$	$c_{\text{Q, E-C1}}$
C2	$\dot{C}_{33} + \dot{C}_{\text{W,Comp2}} + \dot{Z}_{\text{Comp2}} = \dot{C}_{34}$	$c_{\text{W,Comp2}}$
E-C2	$\dot{C}_{34} + \dot{C}_{\text{Q, E-C2}} + \dot{Z}_{E-C2} = \dot{C}_{35}$	$c_{\text{Q,E-C2}}$
RCY-101 and 102	–	$c_{116} = c_{115}, c_{112} = c_{110}$

Table 9 Exergy parameters of components

Component	$E_{\text{F,k}}/(kW)$	$E_{\text{P,k}}/(\text{kW})$	$\epsilon/(\%)$	$E_{\text{D,k}}/(\text{kW})$
Ammonia Reboiler	379.91	97.99	25.79	281.92
E-100	5.44	1.21	22.19	4.23
Ammonia Absorber	4303.82	4273.01	99.28	30.81
P-100	1.88	1.52	80.86	0.36
Ammonia Stripper	4383.73	4361.23	99.48	22.50
Ammonia Condenser	6.35	0.00	0.00	0.49
VLV-100	7.76	0.00	0.00	7.76
Evaporator	40.65	38	93.46	1.77
V-100	8151.25	8249.25	99.98	2.00
V – 1	309.7	303.3	97.93	6.4
C1	78	64.2	82.26	13.83
E-C1	14.2	0.00	2.8	14.16
C2	36	29.0	80.92	6.85
E-C2	5.0	0.00	2.2	4.96
Overall plant	754.01	525.69	69.71	228.31

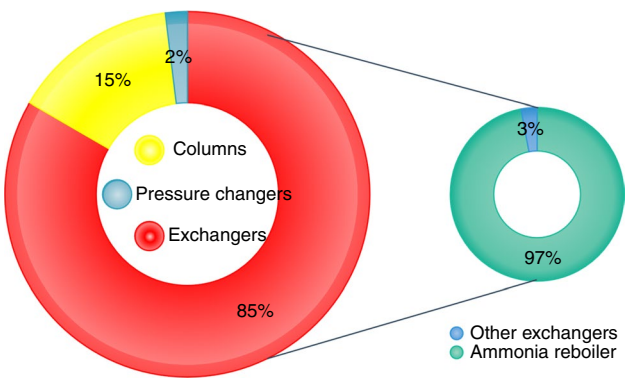

Fig. 4 The Exergy destruction contribution of process equipment

Results and discussion

After conducting process design and simulation of the CO_2 liquefaction cycle and calculating the exergy streams, the measurement parameters of exergy with the aim at comparing of components in the developed system are provided in Table 9 and Fig. 4. It is determined that the main part of the exergy is destructed in the ammonia reboiler, ammonia absorber and stripper columns with the amount of 281.92, *30.8,* and 22.50 kW, respectively. Although the ammonia stripper and absorber have the exergy efficiencies of 99%; the columns mainly destruct exergy owing to the component's separation, chemical reactions, and consumption of considerable thermal energy amounts in the condensers at the top of the columns. Among heat exchangers, the process heat exchanger i.e., E-100 has the highest amount of exergy destruction after the ammonia reboiler. It is a special heat exchanger between the ammonia absorber and stripper columns, and destructs exergy with the amount of 4.23 kW. Coolers and conventional condensers are dissipative components. These components have no useful product in which the generated thermal energy is thrown away and not used anywhere. In these cases, the exergy efficiency is not defined and exergy destruction is just calculated. In the ARS only ammonia condenser, and in the CO_2 compression unit E-C1 as well as E-C2 are considered as dissipative components. For the only expansion valve, as it has no useful output and declines the exergy value of outlet stream, which is in fact equal to the quantity of exergy destructed in the process of refrigerant pressure drop i.e., 7.76 kW; therefore, it associates no valuable product.

Table 10 presents unit exergy cost and cost rates for each stream for the developed ARS. The cost of captured

Table 10 Unit exergy cost and exergy cost of streams

$\dot{C}(\$\ h^{-1})$	c/($\$\ GJ^{-1}$)	Stream No. exergy ($\$\ KJ^{-1}$)
0.00	0.00	101
2134.42	72.03	102
1127.53	72.04	103
1012.63	72.04	104
2118.62	72.97	105
2119.32	72.98	106
2119.92	72.99	107
1143.17	72.86	108
2100.03	72.63	109
2098.61	72.63	110
0.00	0.00	111
2098.61	72.63	112
1140.25	72.78	113
1139.94	72.89	114
1129.27	72.89	115
1129.34	72.89	116
40.71	37.14	30
40.96	37.76	31
59.07	44.90	32
59.21	46.62	33
73.02	53.33	34
72.55	54.10	35
72.55	54.10	36
83.44	56.50	37
0.27	37.76	38

CO_2 from the CCU plant is considered equal to 37.14 $\$\ GJ^{-1}$, and the cost of feed stream i.e., the flue gas from ammonia plant is considered zero. As it can be seen in the presented table the cost rate of captured CO_2 from CCU plant increases by passing through the equipment of the system; particularly compressors.

After performing exergy analysis, the components are exergoeconomically analyzed independently. The significance of each equipment is known from the magnitude of the sum $\dot{Z}_k + \dot{C}_{D,K}$. Therefore, this is a way to model the components of the developed system in terms of their rank. f_k represents the performance of each component of the developed system. The aforementioned values are obtained and presented in Table 11. After the compressors in CO_2 compression unit, the stripper, the absorber, heat exchanger E-100, and evaporator have the highest values of the sum $\dot{Z} + \dot{C}_D$ in the CO_2 liquefaction cycle. The value shows the most important equipment from the exergoeconomic viewpoint.

The factor of exergoeconomic is employed to discover the protruding factor of the cost infliction. It means that when the f_k has a large value, the equipment needs to be checked in terms of capital cost since it looks that the equipment capital cost is very high; therefore, such components are not economically justified. If the f_k has a small value, the components performance needs to be improved, since the components' low-efficiency charges a high expenditure on the system. It can be said that the low amounts of the exergoeconomic factor of the components show that the costs are associated with the amount of exergy destructed in the component. Compressors of CO_2 compression unit have fairly high amount of f_k, and are responsible for the highest value of the sum $\dot{Z} + \dot{C}_D$ as well. This subject recommends that the components have high capital investment and O&M costs which had better be dominated. The potential of cost reduction needs to be explored in order to be justified economically since it

Table 11 The result of exergoeconomic analysis

Equipment	$\dot{Z}/\$\ h^{-1}$	$C_P/\$\ GJ^{-1}$	$C_F/\$\ GJ^{-1}$	$\dot{C}_D/\$\ h^{-1}$	$\dot{E}_D/GJ\ h^{-1}$	$\dot{Z}_D + \dot{C}_D/\$\ h^{-1}$	$f_k/\%$
Reboiler NH3	0.5	22.89	0.00	0.00	1.0149	0.50	100.00
E100	0.48	139.79	72.63	1.11	0.0152	1.59	30.25
Absorber	0.86	38.1	737.24	4.09	0.8443	4.95	17.37
P100	0.27	125.91	21.00	0.03	0.0013	0.30	90.83
Stripper	0.55	72.55	71.95	5.71	0.0815	6.25	8.81
Cond	0.17	0.00	2.92	0.01	0.0018	0.18	97.08
Vlv-100	0	0.00	11.23	0.31	0.0279	0.31	0.00
Evaporator	0.51	80.01	72.89	0.70	0.0095	1.21	42.31
v-100	0.27	72.04	72.03	0.52	0.0072	0.79	34.27
C1	12.21	78.43	21.00	1.05	0.0498	13.26	92.11
E-IC1	0.14	0.00	2.73	0.14	0.0510	0.28	50.15
C2	11.05	134.71	21.00	0.52	0.0247	11.57	95.52
E-IC2	0.17	0.00	14.46	0.42	0.0293	0.59	28.63
V-1	0.26	37.76	36.52	0.84	0.0230	1.10	23.64

appears that the amount of capital cost is so high which leads to losing its economic justification.

Conclusions

Process design and thermoeconomic assessment are conducted for the developed CO_2 liquefaction cycle. The developed CO_2 liquefaction is driven by waste exhaust HR for an industrial CCU plant.

The process modeling of the CO_2 liquefaction cycle is developed and simulated in Aspen Hysys™ v.10 software using Peng-Robinson equation of state. Results of simulation show that the developed CO_2 liquefaction system can liquify CO_2 with the capacity of 54.5 tons per day using of the flue gas enthalpy. Results of thermodynamic analyses show that the CO_2 liquefaction cycle has COP of 0.28 and exergy efficiency of 69.7%. Additionally, the highest amount of exergy is destructed, respectively, in ammonia reboiler and absorber with the amount of 281.92 and 30.8 kW. Exergoeconomic analysis shows that the absorber, the stripper, heat exchanger E-100; and evaporator have the highest values of the sum $\dot{Z} + \dot{C}_D$ among the equipment in the CO_2 liquefaction cycle, and the compressors of CO_2 compression unit have the highest amount of the value among all equipment in the developed system.

Acknowledgements The corresponding authors would like to acknowledge the Iran's National Elite Foundation (INEF) for the financial support [grant number 15.20772]. The technical supports of the Kermanshah Petrochemical Industries Co. and Shahrekord Carbon Dioxide Co. are gratefully acknowledged.

Author contributions R.S.: Conceptualization, Methodology, Software, Formal analysis, Visualization, Writing—Original Draft, Review & Editing. A.A.: Project administration, Supervision, Resources, Review & Editing. R.G.: Project administration, Supervision, Resources, Review & Editing. L.M.R.: Supervision, Conceptualization, Review & Editing. F.P.: Supervision, Methodology, Review & Editing.

References

1. Adams I, Thomas A, Hoseinzade L, Madabhushi PB, Okeke IJ. Comparison of CO_2 capture approaches for fossil-based power generation: review and meta-study. Processes. 2017;5(3):44.
2. Chen Y-H, Shen M-T, Chang H, Ho C-D. Control of solvent-based post-combustion carbon capture process with optimal operation conditions. Processes. 2019;7(6):366.
3. Romeo LM, Minguell D, Shirmohammadi R, Andrés JM. Comparative analysis of the efficiency penalty in power plants of different amine-based solvents for CO_2 capture. Ind Eng Chem Res. 2020;59(21):10082–92. https://doi.org/10.1021/acs.iecr.0c01483.
4. Davarpanah A, Mirshekari B. Experimental study of CO_2 solubility on the oil recovery enhancement of heavy oil reservoirs. J Therm Anal Calorim. 2020;139(2):1161–9. https://doi.org/10.1007/s10973-019-08498-w.
5. Shirmohammadi R, Ghorbani B, Hamedi M, Hamedi M-H, Romeo LM. Optimization of mixed refrigerant systems in low temperature applications by means of group method of data handling (GMDH). J Nat Gas Sci Eng. 2015;26:303–12. https://doi.org/10.1016/j.jngse.2015.06.028.
6. Cansino JM, Sánchez-Braza A, Espinoza N. Moving towards a green decoupling between economic development and environmental stress? A new comprehensive approach for Ecuador. Clim Dev. 2021. https://doi.org/10.1080/17565529.2021.1895701.
7. Broberg Viklund S, Johansson MT. Technologies for utilization of industrial excess heat: potentials for energy recovery and CO_2 emission reduction. Energy Convers Manage. 2014;77:369–79. https://doi.org/10.1016/j.enconman.2013.09.052.
8. Mahmoudan A, Samadof P, Kumar R, Jalili M, Issakhov A. Emergy-based exergoeconomic and exergoenvironmental evaluation of a combined power and cooling system based on ORC-VCR. J Therm Anal Calorim. 2021. https://doi.org/10.1007/s10973-020-10422-6.
9. Naeimi A, Bidi M, Ahmadi MH, Kumar R, Sadeghzadeh M, Alhuyi NM. Design and exergy analysis of waste heat recovery system and gas engine for power generation in Tehran cement factory. Thermal Sci Eng Prog. 2019;9:299–307. https://doi.org/10.1016/j.tsep.2018.12.007.
10. Viklund SB, Johansson MT. Technologies for utilization of industrial excess heat: potentials for energy recovery and CO_2 emission reduction. Energy Convers Manage. 2014;77:369–79.
11. Woolley E, Luo Y, Simeone A. Industrial waste heat recovery: a systematic approach. Sustain Energy Technol Assess. 2018;29:50–9. https://doi.org/10.1016/j.seta.2018.07.001.
12. Saleh S, Pirouzfar V, Alihosseini A. Performance analysis and development of a refrigeration cycle through various environmentally friendly refrigerants. J Therm Anal Calorim. 2019;136(4):1817–30. https://doi.org/10.1007/s10973-018-7809-3.
13. Sharifi S, Nozad Heravi F, Shirmohammadi R, Ghasempour R, Petrakopoulou F, Romeo LM. Comprehensive thermodynamic and operational optimization of a solar-assisted LiBr/water absorption refrigeration system. Energy Rep. 2020;6:2309–23. https://doi.org/10.1016/j.egyr.2020.08.013.
14. Bagheri BS, Shirmohammadi R, Mahmoudi SMS, Rosen MA. Optimization and comprehensive exergy-based analyses of a parallel flow double-effect water-lithium bromide absorption refrigeration system. Appl Therm Eng. 2019;152:643–53. https://doi.org/10.1016/j.applthermaleng.2019.02.105.
15. Golchoobian H, Saedodin S, Ghorbani B. Exergetic and economic evaluation of a novel integrated system for trigeneration of power, refrigeration and freshwater using energy recovery in natural gas pressure reduction stations. J Therm Anal Calorim. 2021. https://doi.org/10.1007/s10973-021-10607-7.
16. Ghorbani B, Ebrahimi A, Skandarzadeh F, Ziabasharhagh M. Energy, exergy and pinch analyses of an integrated cryogenic natural gas process based on coupling of absorption–compression refrigeration system, organic Rankine cycle and solar parabolic trough collectors. J Therm Anal Calorim. 2020. https://doi.org/10.1007/s10973-020-10158-3.
17. Niasar MS, Ghorbani B, Amidpour M, Hayati R. Developing a hybrid integrated structure of natural gas conversion to liquid fuels, absorption refrigeration cycle and multi effect desalination (exergy and economic analysis). Energy. 2019;189:116162. https://doi.org/10.1016/j.energy.2019.116162.
18. Chang Y-I, Wu L-C, Wu C-C, Jang LK. Computer simulation of an ammonia-water absorption cycle for refrigeration: using a distillation tower to replace the generator. Energy Power Eng. 2020;12(06):237.

19. Ghorbani B, Shirmohammadi R, Amidpour M, Inzoli F, Rocco M. Design and thermoeconomic analysis of a multi-effect desalination unit equipped with a cryogenic refrigeration system. Energy Convers Manage. 2019;202:112208. https://doi.org/10.1016/j.enconman.2019.112208.
20. Aliyon K, Mehrpooya M, Hajinezhad A. Comparison of different CO_2 liquefaction processes and exergoeconomic evaluation of integrated CO_2 liquefaction and absorption refrigeration system. Energy Convers Manage. 2020;211:112752.
21. Ghorbani B, Mehrpooya M, Shirmohammadi R, Hamedi MH. A comprehensive approach toward utilizing mixed refrigerant and absorption refrigeration systems in an integrated cryogenic refrigeration process. J Clean Prod. 2018. https://doi.org/10.1016/j.jclepro.2018.01.109.
22. Shirmohammadi R, Soltanieh M, Romeo LM. Thermoeconomic analysis and optimization of post-combustion CO_2 recovery unit utilizing absorption refrigeration system for a natural-gas-fired power plant. Environ Prog Sustain Energy. 2018;37(3):1075–84. https://doi.org/10.1002/ep.12866.
23. Ghorbani B, Hamedi M-H, Amidpour M. Exergoeconomic evaluation of an integrated nitrogen rejection unit with LNG and NGL co-production processes based on the MFC and absorbtion refrigeration systems. Gas Process. 2016;4(1):1–28.
24. Ghorbani B, Shirmohammadi R, Mehrpooya M, Mafi M. Applying an integrated trigeneration incorporating hybrid energy systems for natural gas liquefaction. Energy. 2018;149:848–64.
25. Shirmohammadi R, Aslani A, Ghasempour R. Challenges of carbon capture technologies deployment in developing countries. Sustain Energy Technol Assess. 2020;42:100837. https://doi.org/10.1016/j.seta.2020.100837.
26. Bahadori A. Estimation of combustion flue gas acid dew point during heat recovery and efficiency gain. Appl Therm Eng. 2011;31(8):1457–62. https://doi.org/10.1016/j.applthermaleng.2011.01.020.
27. Somers CM. Modeling Absorption Chillers in ASPEN. ProQuest; 2009.
28. Ghorbani B, Shirmohammadi R, Mehrpooya M. A novel energy efficient LNG/NGL recovery process using absorption and mixed refrigerant refrigeration cycles—economic and exergy analyses. Appl Thermal Eng. 2018. https://doi.org/10.1016/j.applthermaleng.2017.12.099.
29. Bejan A. Advanced engineering thermodynamics. Hoboken, New Jersey: Wiley; 2016.
30. Abdollahpour A, Ghasempour R, Kasaeian A, Ahmadi MH. Exergoeconomic analysis and optimization of a transcritical CO_2 power cycle driven by solar energy based on nanofluid with liquefied natural gas as its heat sink. J Therm Anal Calorim. 2020;139(1):451–73. https://doi.org/10.1007/s10973-019-08375-6.
31. Bejan A, Tsatsaronis G, Moran M, Moran MJ. Thermal design and optimization. Wiley; 1996.
32. Szargut J. Egzergia: poradnik obliczania i stosowania. Wydawnictwo Politechniki Śląskiej; 2007. http://web.mit.edu/2.813/www/readings/APPENDIX.pdf.
33. Mahmoudan A, Samadof P, Sadeghzadeh M, Jalili M, Sharifpur M, Kumar R. Thermodynamic and exergoeconomic analyses and performance assessment of a new configuration of a combined cooling and power generation system based on ORC–VCR. J Therm Anal Calorim. 2020. https://doi.org/10.1007/s10973-020-10230-y.
34. Haydary J. Chemical process design and simulation: Aspen Plus and Aspen Hysys applications. Wiley; 2019.
35. Liu Z, Liu Z, Yang X, Zhai H, Yang X. Advanced exergy and exergoeconomic analysis of a novel liquid carbon dioxide energy storage system. Energy Convers Manage. 2020;205:112391. https://doi.org/10.1016/j.enconman.2019.112391.
36. Charoensuppanimit P, Kitsahawong K, Kim-Lohsoontorn P, Assabumrungrat S. Incorporation of hydrogen by-product from NaOCH3 production for methanol synthesis via CO_2 hydrogenation: process analysis and economic evaluation. J Clean Prod. 2019;212:893–909. https://doi.org/10.1016/j.jclepro.2018.12.010.
37. Ekrataleshian A, Pourfayaz F, Ahmadi MH. Thermodynamic and thermoeconomic analyses and energetic and exergetic optimization of a turbojet engine. J Therm Anal Calorim. 2020. https://doi.org/10.1007/s10973-020-10310-z.
38. Liu Z, He T. Exergoeconomic analysis and optimization of a gas turbine-modular helium reactor with new organic rankine cycle for efficient design and operation. Energy Convers Manage. 2020;204:112311. https://doi.org/10.1016/j.enconman.2019.112311.
39. Talebizadehsardari P, Ehyaei MA, Ahmadi A, Jamali DH, Shirmohammadi R, Eyvazian A, et al. Energy, exergy, economic, exergoeconomic, and exergoenvironmental (5E) analyses of a triple cycle with carbon capture. J CO2 Util. 2020;41:101258. https://doi.org/10.1016/j.jcou.2020.101258.
40. Wang Y, Liu Y, Liu X, Zhang W, Cui P, Yu M, et al. Advanced exergy and exergoeconomic analyses of a cascade absorption heat transformer for the recovery of low grade waste heat. Energy Convers Manage. 2020;205:112392. https://doi.org/10.1016/j.enconman.2019.112392.